Supplementary Appendix

Supplement to: Marfella R, Prattichizzo F, Sardu C, et al. Microplastics and nanoplastics in atheromas and cardiovascular events. N Engl J Med 2024;390:900-10. DOI: 10.1056/NEJMoa2309822

This appendix has been provided by the authors to give readers additional information about the work.

TABLE OF CONTENTS

Supplementary Methods

Sample size calculation

There is no prior information by which to gauge our sample size. Therefore, we performed an interim analysis that included the first 100 patients to calculate the sample size needed for our study. We observed that 61 subjects (61%) had evidence of micronanoplastics (MNPs) with a 2.1 increased risk for the outcome compared with patients without any trace of MNPs. Considering an alpha of 0.05, a beta of 0.2, a baseline event rate of 9 events/100 person-years in the group without evidence of MNPs, and a planned follow-up of 3 years, the proportional-hazards regression model (**1**) yielded a sample size of 246 patients. Considering an expected 20% loss at follow-up, we set a target of 300 patients to be enrolled after screening.

Detection and quantitation of microplastics by pyrolosis-gas chromatography-mass spectroscopy (Py-GC/MS)

For our study, we used the following for plastic reference standards: Frontier Laboratories Ltd (Japan) provided the microplastics-silicon dioxide (MPs-SiO_2) calibration standard. The commercial mixture contained 11 of the most common types of plastics, including polyethylene, polypropylene, polystyrene, acrylonitrile butadiene styrene copolymer, styrene-butadiene copolymer, polymethyl methacrylate, polycarbonate, polyvinylchloride, polyethylene terephthalate, Nylon 6, and Nylon 66. Analytical grade dichloromethane and hexane were supplied from Merck (Darmstadt, Germany).

The biological samples were pre-treated before analysis. To avoid water interferences during the analysis, an aliquot of 100 mg of each sample was carefully freeze-dried. All samples were stored in glass vials at room temperature. Then, 1 mg of the freeze-dried sample was placed in the pyrolysis cup, covered with quartz wool and analyzed (**2**). All pyrolysis cups were new and free from any possible contaminants.

Identification and quantification of microplastics were performed by Py-GC/MS in a system equipped with a Multi-Shot EGA/PY-3030D micro-furnace pyrolizer (Frontier Laboratories Ltd.) and coupled to a GC 7890 gas chromatograph with an MSD 5975C triple quadrupole mass spectrometry detector (Agilent Technologies). Pyrolysis of the sample was performed using the single-shot mode at 600 °C for 0.20 minutes (12 seconds), and the pyrolyzates were analyzed by the GC/MS system. Both the pyrolyzer interface and GC injector temperatures were set at 300 °C. The samples were injected with a split of 50:1 on a stainless-steel Ultra Alloy® 5 capillary column (30 m, 0.25 mm I.D., 0.25 μm film thickness) provided by Frontier Lab. The GC oven column temperature program was set with the following parameters: held at 40 °C for 5 minutes, with a ramp to 320 °C at 20 °C $minutes^{-1}$, and held for 20 minutes. Helium was used as the carrier gas at a 1.0 ml/minutes. The detector ion source temperature was set at 230 °C with an ionization voltage of 70 eV, leading to an ionization and fragmentation of the molecules [16]. Scan modality was used with a mass range from 35 to 650 *m*/*z*, operating at 2 scans/s (**2**). The results were interpreted using the F-Search MPs (Frontier Lab Ltd.), which contains pyrolyzates and polymers libraries, leading to a qualitative and quantitative analysis of microplastics. For the preparation of the calibration curves, different amounts (0.4, 2.0, and 4.0 mg) of the standard mixture (MPs-SiO_2) were weighted to the pyrolysis cup (80 μL) and covered with quartz wool before analysis by Py-GC/MS.

To minimize sample contamination, the entire process was implemented with quality assurances and quality control steps. All laboratory procedures were conducted under a fume hood, by using laboratory glassware and plastic free equipment. Cotton coats were worn during the procedures. All working surfaces were cleaned with an ethanol solution prior to starting experiments. Sample blank analyses were carried out before starting each pyrolysis-GC/MS run. The blank consisted in the analysis of a pyrolysis cup, covered with quartz wool. If a blank signal was found, this step made it possible to make corrections for background contamination (**3**). To minimize background pollution from the environment, contact between the plastics and the equipment used in the experiment was avoided as much as possible. In addition, the ultrapure water was filtered using a stainless-steel sieve. The glass test tubes, and glass pipette were washed three times with ultrapure water and oven-dried before use.

Validation of the Pyr-GC/MS method was done in terms of linearity, limit of detection (LOD), and limit of quantification (LOQ). According to literature (**4**), these parameters were calculated for each plastic polymer using the corresponding calibration curves and applying Eqs. (1) and (2), respectively:

$$LOD = 3.3\ x\ \frac{\alpha}{S} \qquad (1)$$

$$LOQ = 10\ x\ \frac{\alpha}{S} \qquad (2)$$

where α is the residual standard deviation of the regression equation, while S is the slope of the calibration curve. Frontier Laboratories Ltd (Japan) provided the commercial mixture containing 11 of the most common types of plastics. The validation results are reported in the table below. Collectively, the performances of the method were satisfactory. A good linearity range was obtained for all the plastic polymers.

Validation parameters of the 11 target plastic polymers.

Polymer	Characteristic pyrolyzate	Indicator ion (m/z)	R^2	LOD (ng)	LOQ (ng)
PE	1,20-Heneicosadiene (C21)	82	0.9947	168.17	509.61
PP	2,4-Dimethyl-1-heptene	70	0.9994	17.22	52.19
PS	Styrene trimer	91	0.9536	0.80	2.42
ABS	2-Phenethyl-4-phenylpent-4-enenitrile	170	0.9316	1.95	5.90
SBR	4-Phenylcyclohexene	104	0.9937	4.08	12.35
PMMA	Methyl methacrylate	100	0.9987	0.12	0.37
PC	p-Isopropenylphenol	134	0.9996	0.20	0.61
PVC	Naphthalene	128	0.9992	3.86	11.69
PET	Benzophenone	182	0.9753	29.06	88.07
N6	Ɛ-caprolactam	116	0.9992	4.70	14.24
N66	Cyclopentanone	84	0.9999	1.96	5.94

LOD denotes limit of detection, LOQ limit of quantification, PE polyethylene, PP polypropylene, PS polystyrene, ABS acrylonitrile butadiene styrene copolymer, SBR styrene-butadiene copolymer, PMMA polymethyl methacrylate, PC polycarbonate, PVC polyvinylchloride, PET polyethylene terephthalate, N6 Nylon 6 and N66 Nylon 66.

Electron microscopy

Carotid fragments obtained during surgery were fixed with 2.5 % glutaraldehyde in phosphate buffer and post-fixed in 0.5 % osmium tetroxide in the same buffer and then dehydrated in an acetone series. Part of the material was subsequently embedded in Epon-Araldite resin for transmission electron microscopy (TEM), and the other part completely dehydrated with hexamethyldisilazane (HMDS) for scanning electron microscopy (SEM) analysis. Sixty nanometer thick sections mounted on copper grids were observed at 80 KV in a Transmission Electron Microscope (Philips CM10).

After imaging, the same grids were coated for 10 seconds with platinum in a sputter coater (Jeol JFC-2300HR) and placed in an aluminum stub for SEM analysis (Jeol JSM-IT800). Low vacuum back scattered electrons images were obtained at 5 KV. X-ray spectra were acquired in the same condition for 30 seconds, elements were automatically detected using the JEOL SEM CENTER software.

Samples processed for SEM were coated for 10 seconds with platinum placed on a stub and imaged in high vacuum either using SED or scanner block electron detector (SBED;, when unusual particles were found, an energy-dispersive X-ray analysis (EDX) detector was used and X-ray spectra acquired as maps of elements and as a total content of element in an area in order to make a direct comparison of element content in particles and amorphous matrix.

Stable isotopes analysis

For isotopic analysis, atherosclerotic plaques were freeze-dried and weighed in tin capsules (approximately 1.5 mg of each sample). Stable carbon and nitrogen ratios were performed at the iCONA lab of the University of Campania Luigi Vanvitelli, by means of an Isotopic Ratio Mass Spectrometer (IRMS Delta Advantage, Thermo Scientific), coupled with an Elemental Analyzer (Flash EA 1112 series, Thermo Scientific), via Continuous Flow Interface (Conflo IV, Thermo Scientific). The analysis is based on the separation of the lighter and heavier isotopes, and the measurement of their relative abundance (**5**). In addition, the methodology permitted the analysis of carbon and nitrogen concentrations in plaque samples.

The resulting measurements were calibrated using international standards with certified isotopic values, aiming to set their values on internationally referenced scales (**6**). The standards used were: IAEA N2 (ammonium sulfate, $\delta^{15}N$ = 20,3‰), Sirfer Yest (yeast, $\delta^{15}N$ = -1,24‰, $\delta^{13}C$ = -20,02‰) and IAEA CH3 (cellulose, $\delta^{13}C$ = -24,724‰). Standard deviations on the repeated measurements of the used standards were: 0,1‰ for $\delta^{13}C$ and 0,2‰ for $\delta^{15}N$.

Plaque phenotyping

For ELISA experiments, protein extraction was performed with 2D lysis buffer (7 mM urea, 2 mM thiourea, 30 mM Tris-HCl pH 8.8, 4% CHAPS [3-([3-cholamidopropyl] dimethylammonium)-1-propane sulfonate]) on plaques cut into small pieces. Tissue was homogenized with a Precellys 24 system (Bertin Technologies) and then centrifuged at 800 x *g* for 10 minutes at 4°C to collect the supernatant. Protein content was determined using the Protein assay dye reagent (5000006, Bio-Rad, Hercules, CA, USA), according to the manufacturer's protocol, and compared with a bovine serum albumin (BSA) standard curve. Levels of cytokines (Interleukin [IL]-18, IL-1β, IL-6, and tumor necrosis factor-α) in plaque extracts were assessed by ELISA assays (IL-18, ab215539, lot GR3446262-1, Abcam, Cambridge, UK; IL-1β, ab214025, lot GR3454388-1, Abcam, Cambridge, UK; IL-6, LF-EK0260, lot SMA113102, AbFrontier, Seoul, Korea; TNF-α, LF-EK0193, lot RJL142307, AbFrontier, Seoul, Korea), following the manufacturer's protocols. The optical density (O.D.) at 450 nm was detected using a microplate reader (model 680, Bio-Rad, Hercules, CA, USA), while the concentration of samples derived by interpolation from each standard curve. The cytokine content was normalized to homogenized tissue weight.

Formalin-fixed specimens of plaque were used for immunohistochemistry and evaluation of collagen content. Deparaffinized and rehydrated sections were subjected to antigen retrieval by adding a buffer containing 10 mM sodium citrate with 0.05% Tween-20, at pH 6.0. Subsequently, the sections were washed in phosphate buffered saline (PBS) and then treated with a blocking solution consisting of fetal bovine serum with 0.1 g/mL saponin for 1 hour at room temperature. Serial sections were then incubated with anti-CD68 (CONFIRM KP-1, 790-2931, Roche) and anti-CD3 (CONFIRM monoclonal 2GV6, 790-4341, Roche) for immunohistochemistry analysis. Quantification was performed using a personal computer-based 24-bit color image analysis system (IM500; Leica Microsystem AG) to evaluate the results. For collagen content assessment, the sections were stained with Sirius Red and observed under polarized light after being mounted on coverslips. Images were captured with identical exposure settings for each section. The results are expressed as the percentage of positivity, using the same quantification system.

References for Supplementary Methods

1. Schoenfeld DA. Sample-size formula for the proportional-hazards regression model. Biometrics 1983;39:499-503.
2. Bouzid N, Anquetil C, Dris R, Gasperi J, Tassin B, Derenne S. Quantification of Microplastics by Pyrolysis Coupled with Gas Chromatography and Mass Spectrometry in Sediments: Challenges and Implications. Microplastics 2022;1:229-239.
3. Okoffo ED, Rauert C, Thomas KV. Mass quantification of microplastic at wastewater treatment plants by pyrolysis-gas chromatography-mass spectrometry. The Science of the total environment 2023;856:159251.
4. Lou F, Wang J, Sima J, Lei J, Huang Q. Mass concentration and distribution characteristics of microplastics in landfill mineralized refuse using efficient quantitative detection based on Py-GC/MS. J Hazard Mater. 2023 Oct 5;459:132098.
5. Ricci P, Sirignano C, Altieri S, Pistillo MG, Santoriello A, Lubritto C. Paestum dietary habits during the Imperial period: archaeological records and stable isotope measurement. Acta Imeko 2016;5:26-32.
6. Birch QT, Potter PM, Pinto PX, Dionysiou DD, Al-Abed SR. Isotope ratio mass spectrometry and spectroscopic techniques for microplastics characterization. Talanta 2021;224:121743.

Supplementary Figure S1. Design of the study.

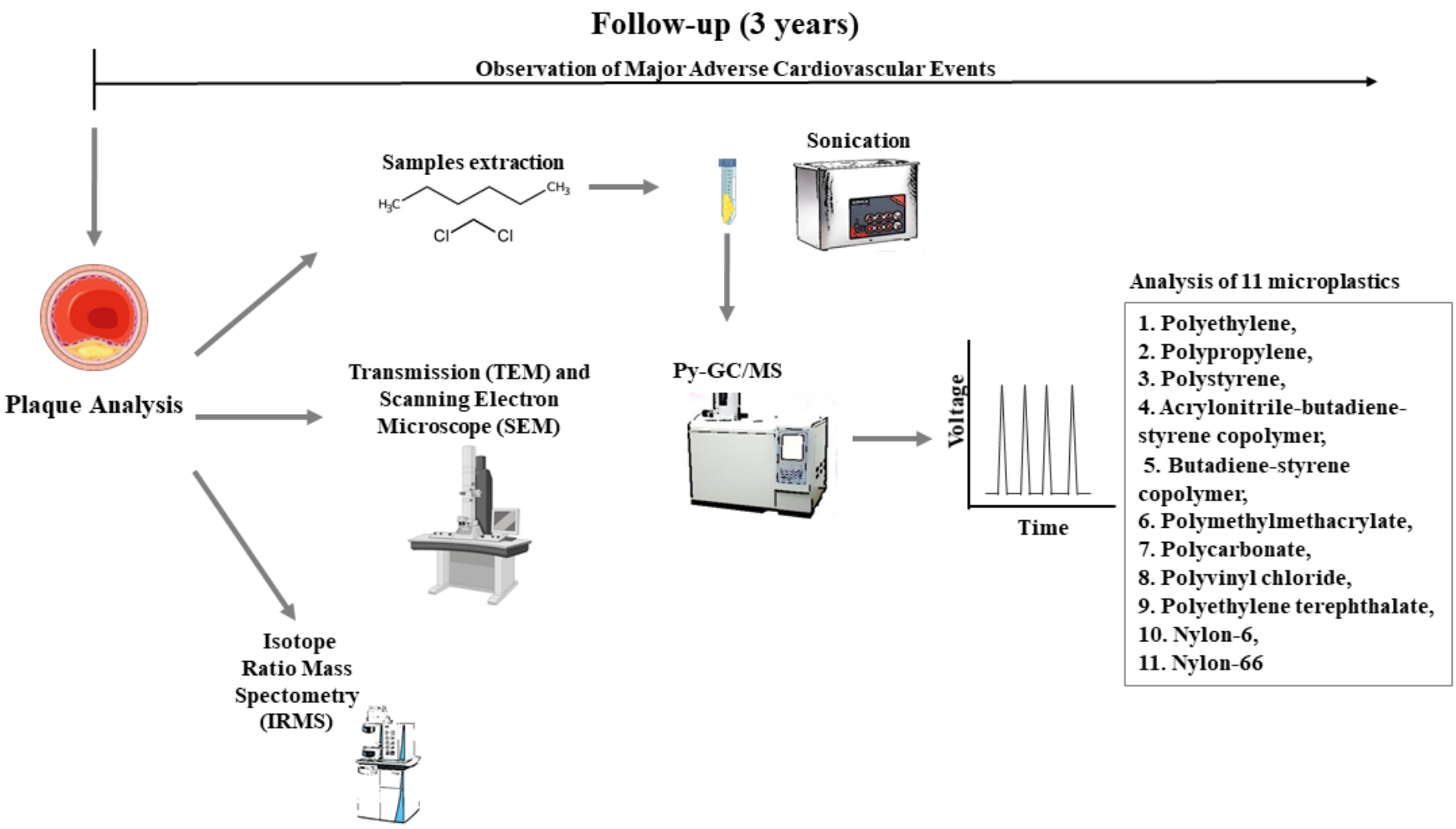

Consecutive patients unergoing carotid endarterectomy were enrolled in the study. After enrollment and during follow-up, specimens of the carotid bifurcation region were studied through Py-GC/MS to quantify 11 different microplastics. Samples from 10 patients were also analyzed by electron microscopy (SEM and TEM) while 26 specimens were analyzed by stable isotope analysis. Patients included in the study were followed to monitor the incidence of non-fatal myocardial infarction, non-fatal stroke, and all-cause mortality for 3 years. Patients were divided into two groups for analysis of clinical outcomes: those with or without evidence of MNPs within the plaque.

Figure S2. Proportion of individuals with MNPs among different centers of recruitment (A) and areas of living (B).

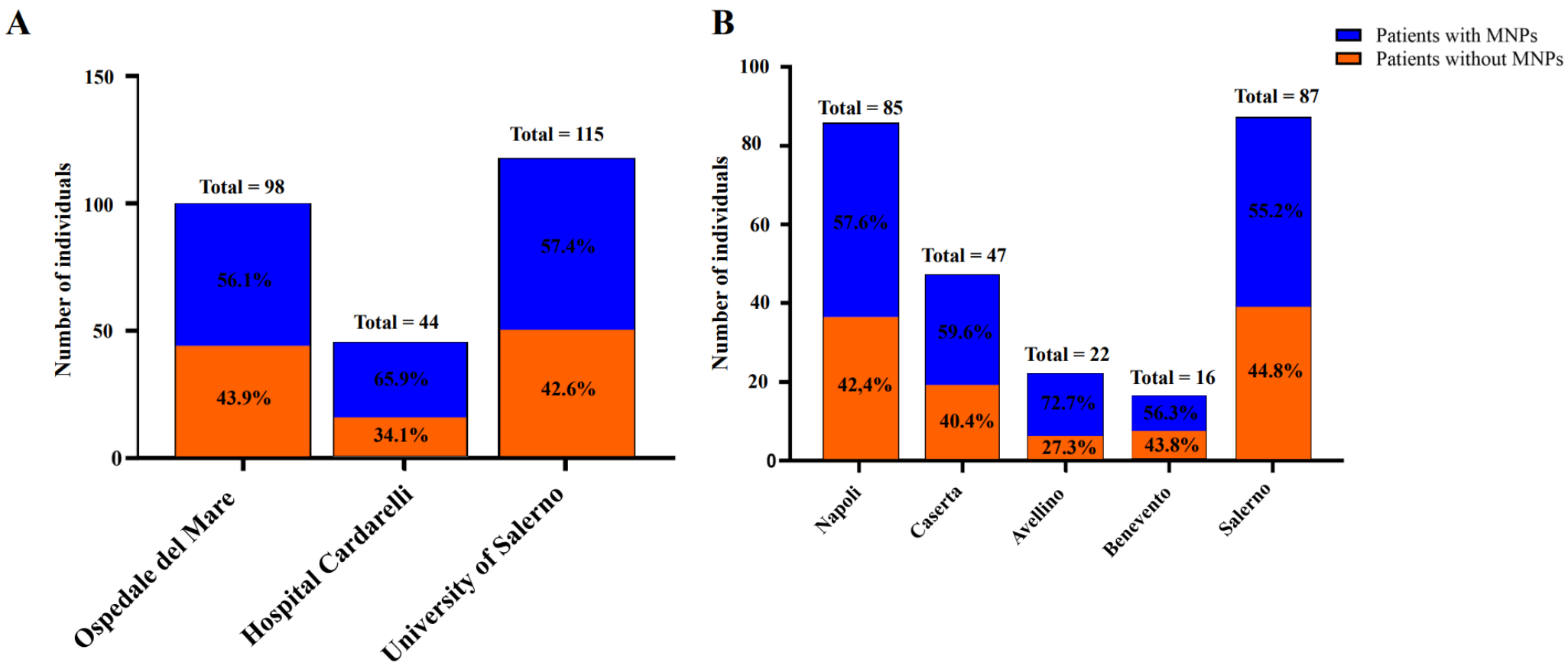

Histograms shows the number and percentage of patients with our without evidence of micronanoplastics (MNP)s within the plaque among the 3 centers that recruited patients for the study (A) or according to the patients' area of living (B). No apparent differences between the groups were observed for either the recruitment center or the patient's area of living according to Fisher's exact test**.**

Figure S3A. Lower magnification of the trasmission electron microscopy (TEM) image of the atheroma showing living cells with vacuoles dispersed in the plaque (relative to Figure 2A).

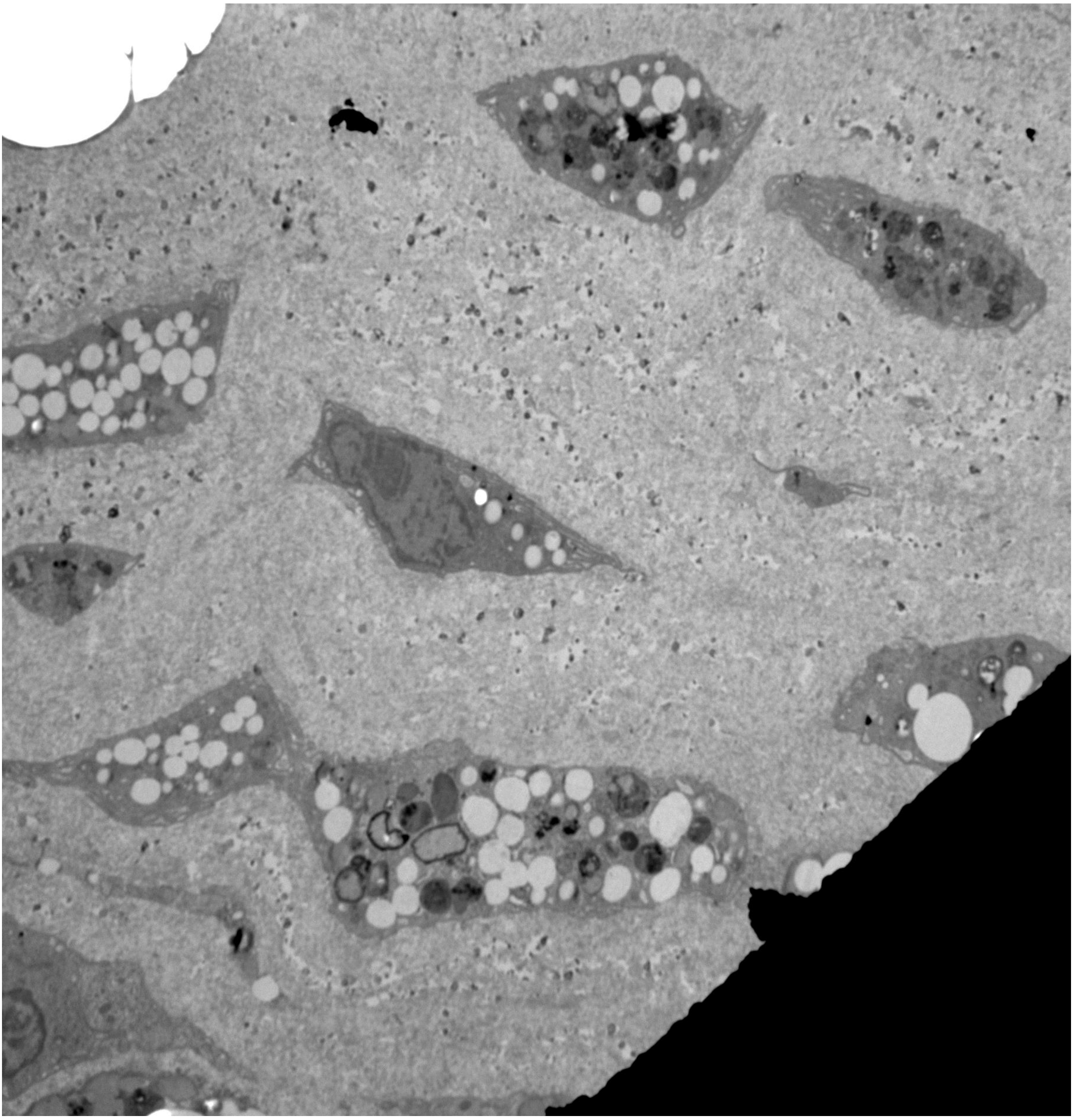

The identified foreign particles had a very electron dense rim, possibly due to the post fixation step with osmium tetroxide. Indeed, we observed a very thin slice of material that was embedded in epoxy resin; thus, we reason that the osmium was only reacting with the surface of the particles.

Figure S3B. X-ray spectra relative to the particles evidenced in the red boxes of Figure 2B. X-ray spectra were calculated and mapped for the whole image and for 2 smaller boxes, one depicted in blue comprising the particle and another identical area nearby that did not contain any visible particle. A list of elements detected in these boxes is shown.

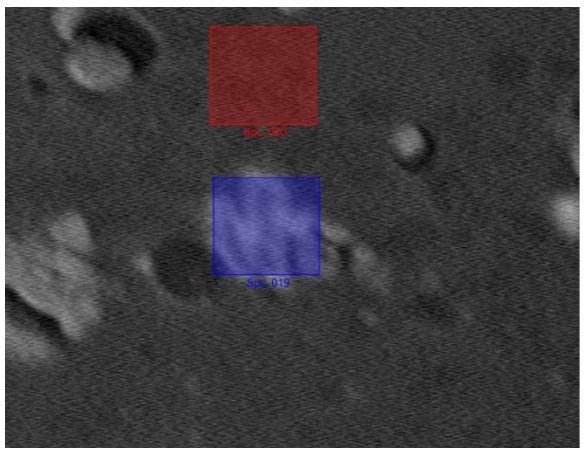

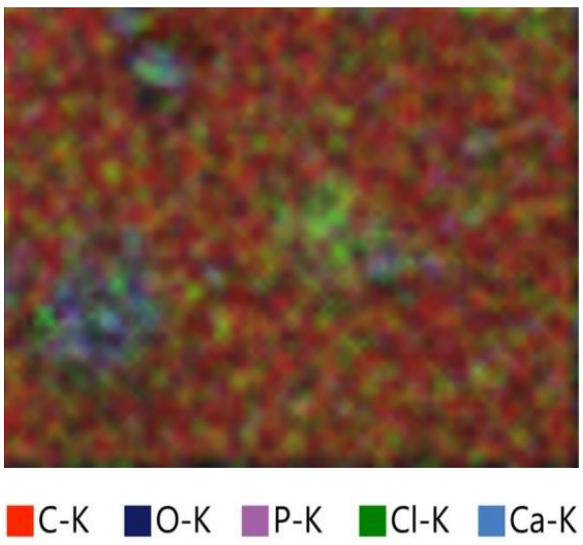

Display name	Standard data	Quantification method	Result Type
Spc_020	Standardless	ZAF	Metal

Element	Line	Mass%	Atom%
C	K	52.66±0.15	72.82±0.20
O	K	16.74±0.17	17.38±0.18
Al	K	11.18±0.21	6.88±0.13
P	K	0.29±0.14	0.15±0.08
Cl	K	2.97±0.20	1.39±0.09
Ca	K	nd	nd
Pt	M	16.16±0.66	1.38±0.06
Total		100.00	100.00
Spc_020			Fitting ratio 0.1730

Display name	Standard data	Quantification method	Result Type
Spc_019	Standardless	ZAF	Metal

Element	Line	Mass%	Atom%
C	K	45.95±0.14	69.15±0.21
O	K	16.20±0.17	18.30±0.19
Al	K	10.23±0.20	6.85±0.14
P	K	1.19±0.17	0.70±0.10
Cl	K	4.65±0.24	2.37±0.12
Ca	K	1.70±0.72	0.77±0.32
Pt	M	20.09±0.72	1.86±0.07
Total		100.00	100.00
Spc_019			Fitting ratio 0.1776

Display name	Standard data	Quantification method	Result Type
Spc_010	Standardless	ZAF	Metal

Element	Line	Mass%	Atom%
C	K	52.11±0.07	71.50±0.10
O	K	17.87±0.09	18.41±0.09
Al	K	11.60±0.11	7.08±0.07
P	K	0.28±0.07	0.15±0.04
Cl	K	2.92±0.10	1.35±0.05
Ca	K	0.69±0.33	0.28±0.14
Pt	M	14.54±0.33	1.23±0.03
Total		100.00	100.00
Spc_010			Fitting ratio 0.1753

Display name	Standard data	Quantification method	Result Type
Spc_009	Standardless	ZAF	Metal

Element	Line	Mass%	Atom%
C	K	45.97±0.07	70.04±0.10
O	K	15.73±0.08	17.99±0.09
Al	K	10.57±0.10	7.17±0.07
P	K	0.50±0.08	0.30±0.05
Cl	K	3.75±0.11	1.94±0.06
Ca	K	0.99±0.34	0.45±0.15
Pt	M	22.48±0.37	2.11±0.03
Total		100.00	100.00
Spc_009			Fitting ratio 0.1772

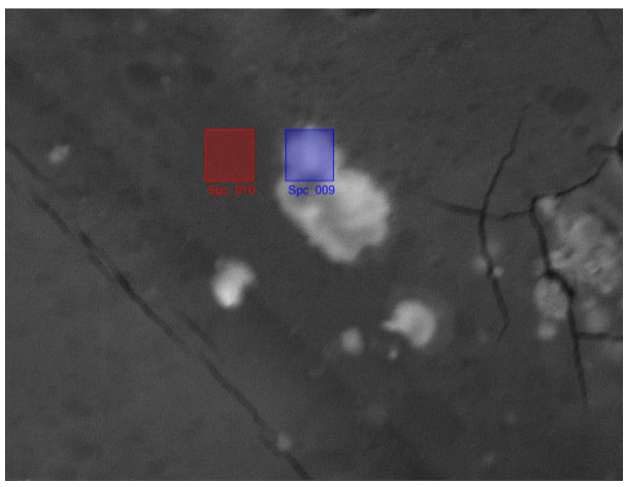

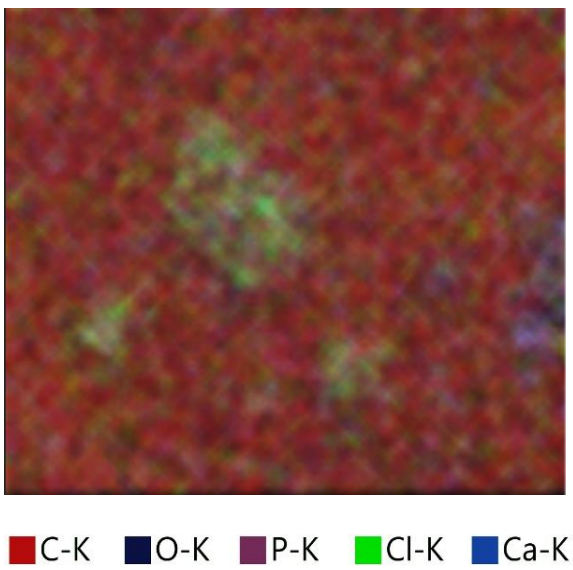

ZAF (atomic number, absorption, fluorescence correction) takes into account the following three effects on the characteristic X-ray intensity when performing quantitative analysis: 1) atomic number (Z) effect, 2) absorption (A) effect, and 3) fluorescence excitation (F) effect.

Fitting ratio is measured as the ratio between the integral of the residual spectrum that remains after peak fitting of the complete X-ray families of the known constituents and the integral of the acquired spectra.

In the spectra, peaks are identified by the name of the element followed by the specific K-, L- and M- shell emission lines. CKa denotes Carbon emission lane Ka, CaLa Calcium emission lane La, OKa Oxygen emission lane Ka, AlKa Aluminum emission lane Ka, PtMz Platinum emission lane Mz, PKa Phosphorous emission lane Ka, PtMa Platinum emission lane Ma, PtMb Platinum emission lane Mb, PtMr Platinum emission lane Mr, ClKa Chlorine emission lane Ka, ClKb Chlorine emission lane Kb, PtM1 Platinum emission lane M1, CaKa Calcium emission lane Ka, CaKb Calcium emission lane Kb.

Figure S3C. X-ray spectra were calculated and mapped for the boxes depicted in blue and red in an area not containing any visible particles to show the contents of the homogeneous area of the plaque that did not contain any particles. A list of elements detected in these boxes is shown.

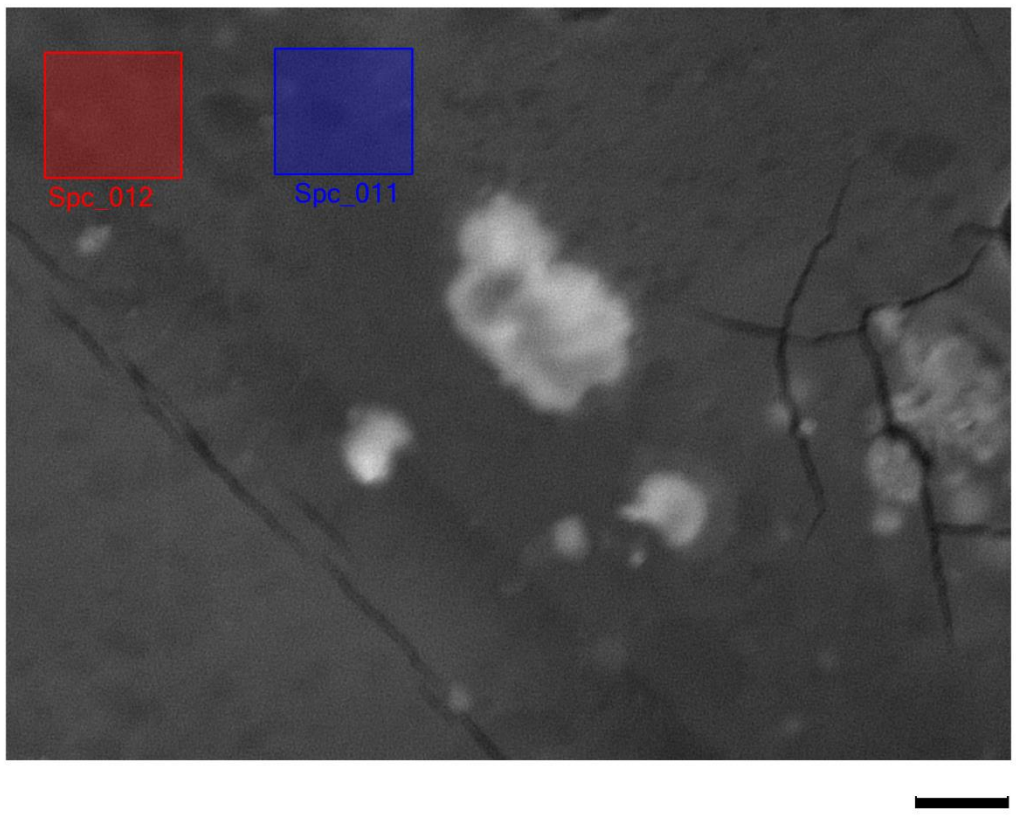

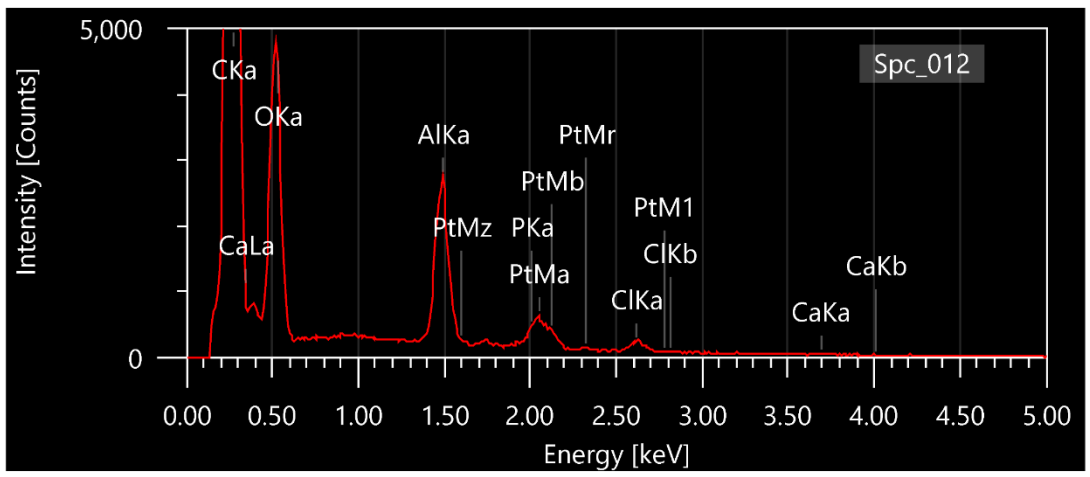

Display name	Standard data	Quantification method	Result Type
Spc_012	Standardless	ZAF	Metal

Element	Line	Mass%	Atom%
C	K	52.87±0.07	71.97±0.10
O	K	17.40±0.09	17.79±0.09
Al	K	11.51±0.11	6.97±0.07
P	K	1.10±0.08	0.58±0.04
Cl	K	3.03±0.10	1.40±0.05
Ca	K	0.32±0.31	0.13±0.13
Pt	M	13.76±0.32	1.15±0.03
Total		100.00	100.00
Spc_012			Fitting ratio 0.1690

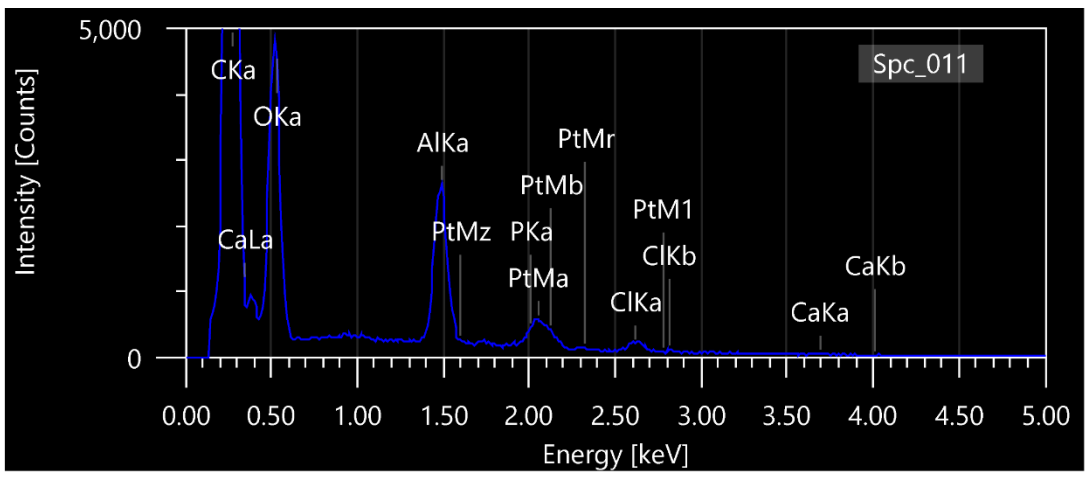

Display name	Standard data	Quantification method	Result Type
Spc_011	Standardless	ZAF	Metal

Element	Line	Mass%	Atom%
C	K	52.11±0.07	71.39±0.10
O	K	17.62±0.09	18.12±0.09
Al	K	11.29±0.11	6.88±0.06
P	K	0.80±0.07	0.42±0.04
Cl	K	2.86±0.10	1.33±0.05
Ca	K	1.74±0.34	0.71±0.14
Pt	M	13.58±0.32	1.15±0.03
Total		100.00	100.00
Spc_011			Fitting ratio 0.1743

ZAF (atomic number, absorption, fluorescence correction) takes into account the following three effects on the characteristic X-ray intensity when performing quantitative analysis: 1) atomic number (Z) effect, 2) absorption (A) effect, and 3) fluorescence excitation (F) effect.

Fitting ratio is measured as the ratio between the integral of the residual spectrum that remains after peak fitting of the complete X-ray families of the known constituents and the integral of the acquired spectra.

In the spectra, peaks are identified by the name of the element followed by the specific K-, L- and M- shell emission lines. CKa denotes Carbon emission lane Ka, CaLa Calcium emission lane La, OKa Oxygen emission lane Ka, AlKa Aluminum emission lane Ka, PtMz Platinum emission lane Mz, PKa Phosphorous emission lane Ka, PtMa Platinum emission lane Ma, PtMb Platinum emission lane Mb, PtMr Platinum emission lane Mr, ClKa Chlorine emission lane Ka, ClKb Chlorine emission lane Kb, PtM1 Platinum emission lane M1, CaKa Calcium emission lane Ka, CaKb Calcium emission lane Kb.

Figure S3D. Scanning electron microscopy (SEM, secondary electrons only) and energy dispersive X-ray (EDX) analysis (K emission lines for Carbon C, Oxigen O, Chlorine Cl and Calcium CA) of a particle dispersed in the atheromatous plaque.

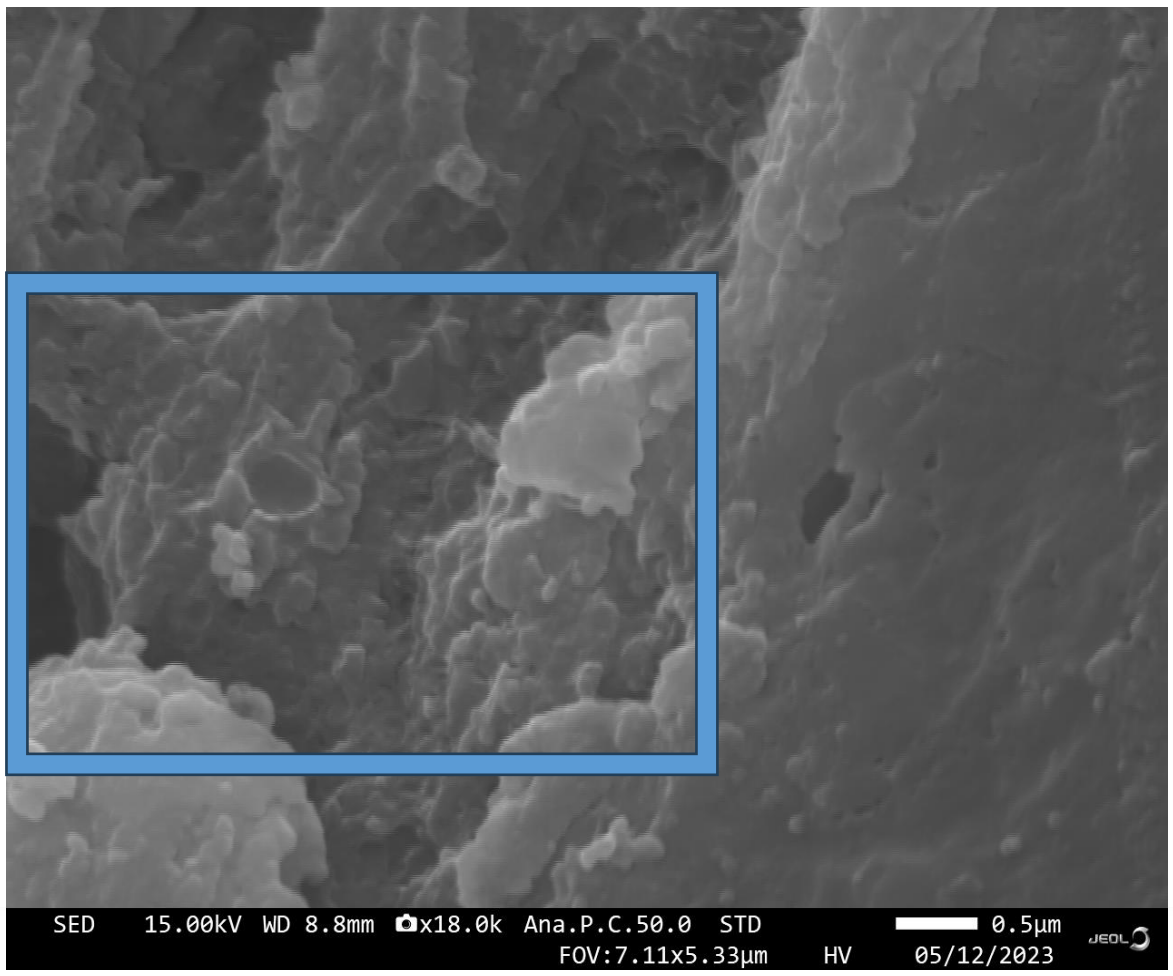

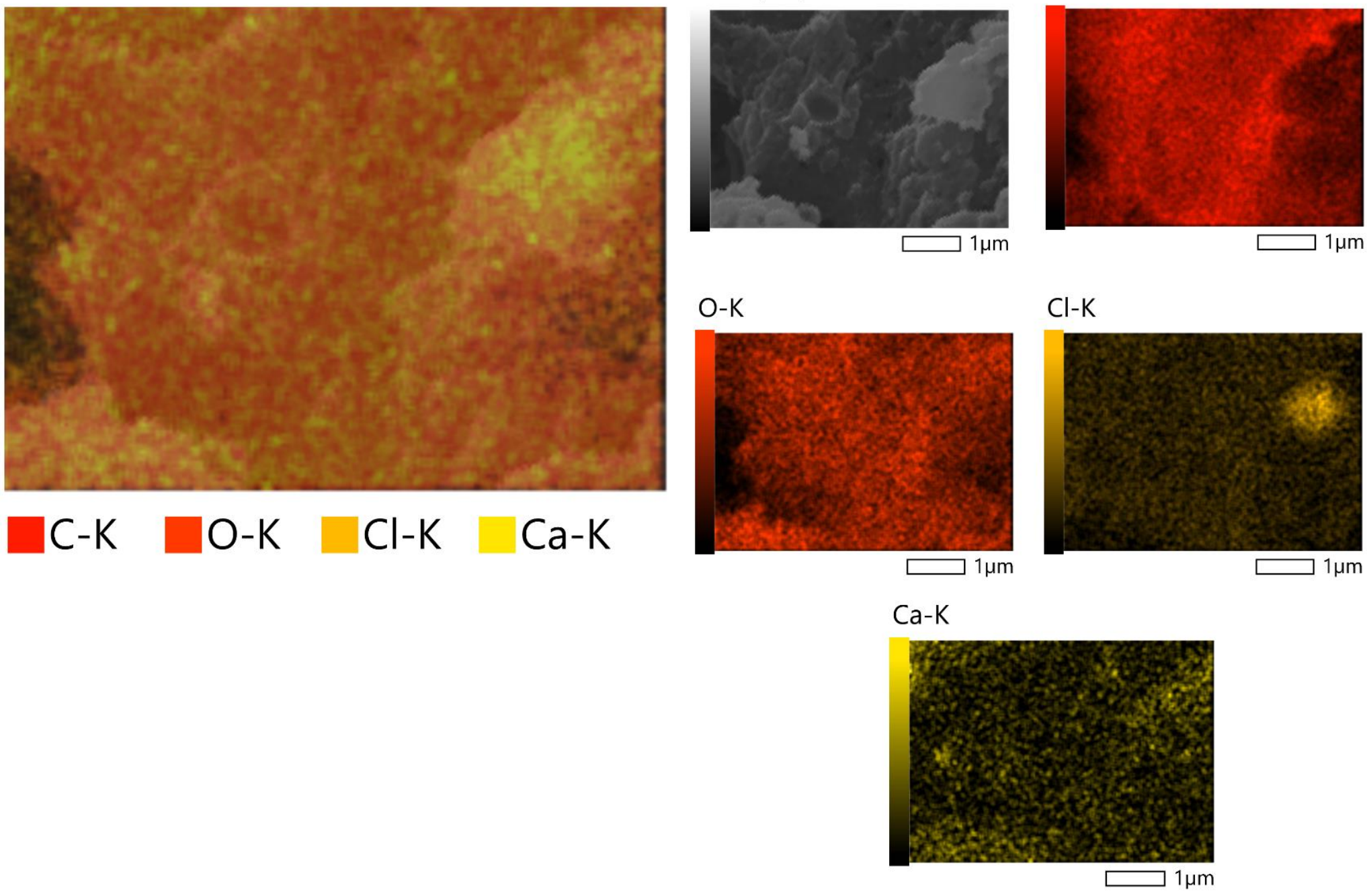

Another example of a particle dispersed in the plaque and analyzed through EDX. Chlorine content is particularly elevated.

Figure S4. Stable isotopes analysis.

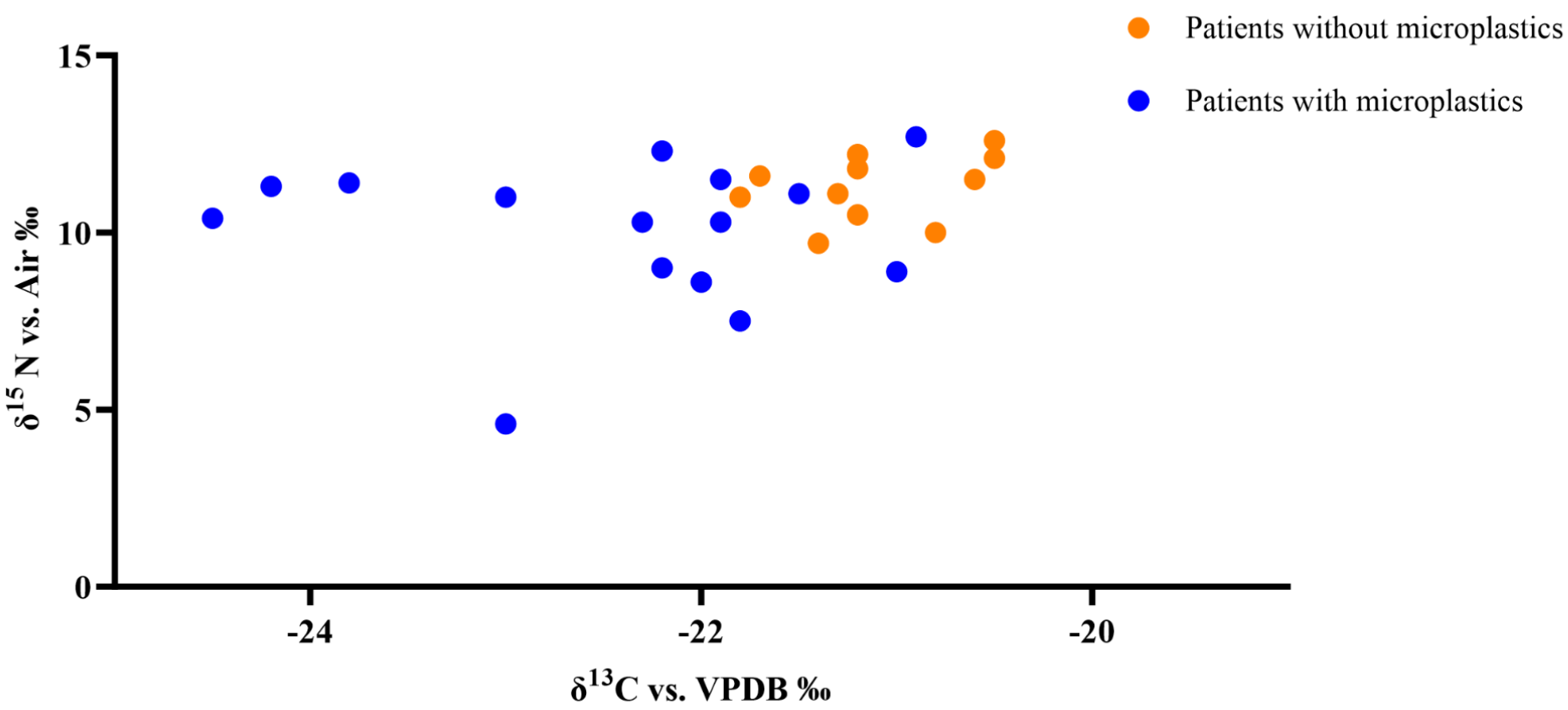

$\delta^{13}C$ vs. $\delta^{15}N$ bi-plot of the analysed atherosclerotic plaques combined with information coming from pyrolysis-gas chromatography-mass spectroscopy. d13C vs VPDB denotes carbon isotopic ratio expressed with delta notation in per mil, measured versus the primary international reference standard Vienna Pee Dee Belemnite (VPDB). d15N vs Air denotes nitrogen isotopic ratio expressed with delta notation in per mil, measured versus the primary international reference standard Air. $\delta^{13}C$ denotes the isotope carbon-13, $\delta^{15}N$ nitrogen-15.

Figure S5. Relationship between micronanoplastics levels and plaque biomarkers.

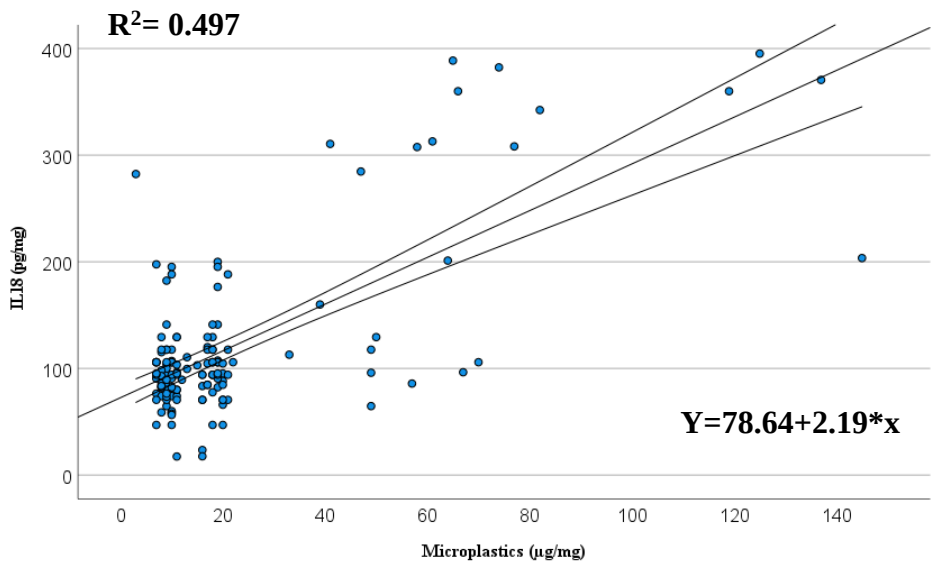

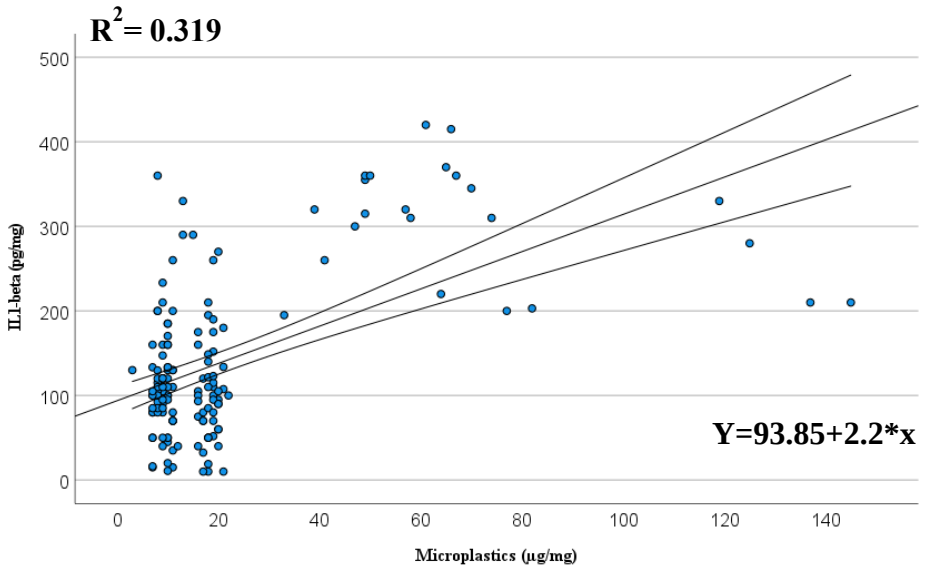

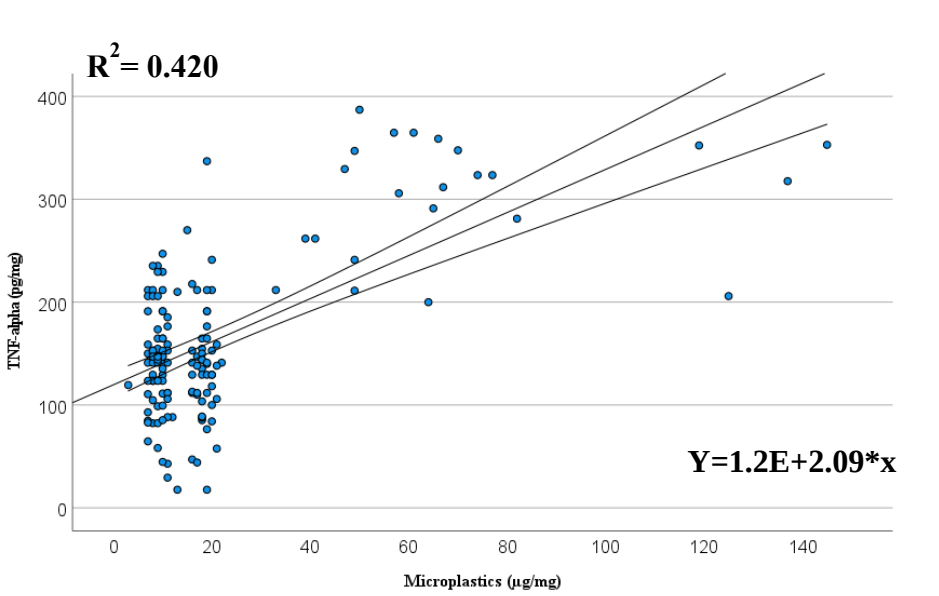

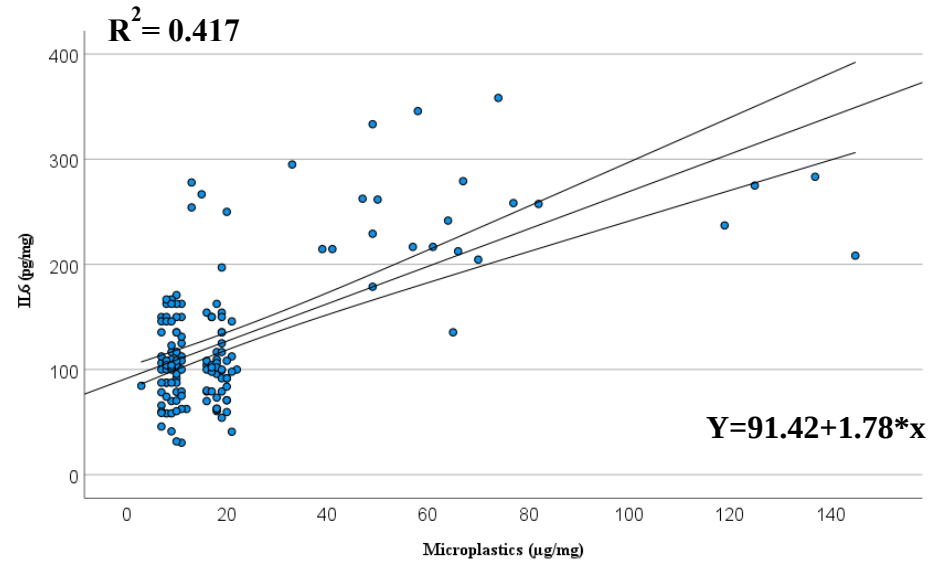

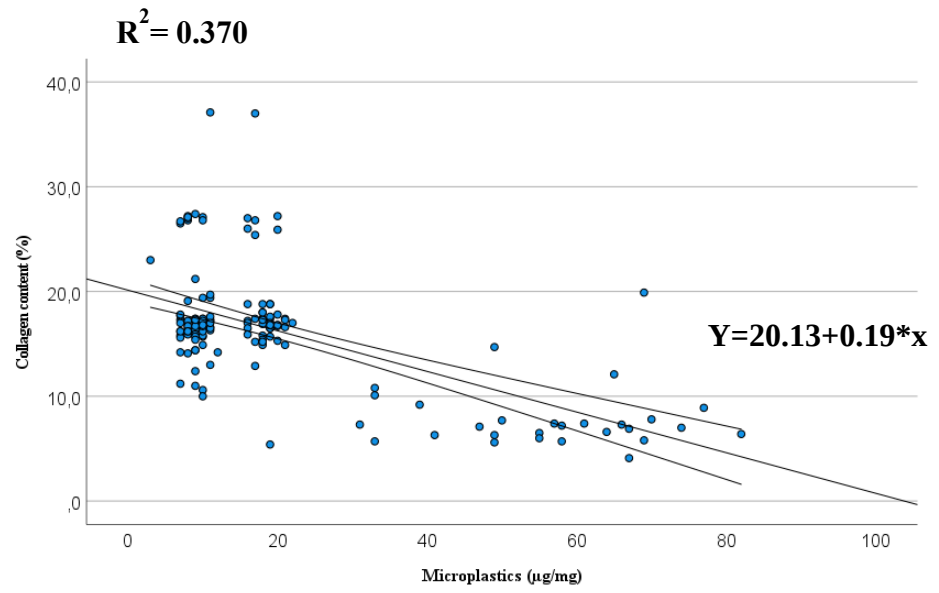

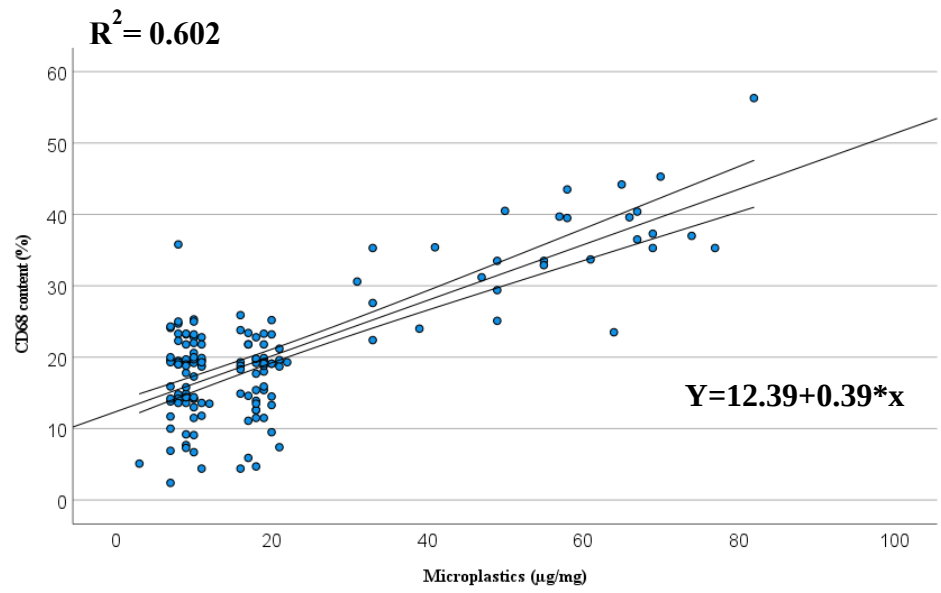

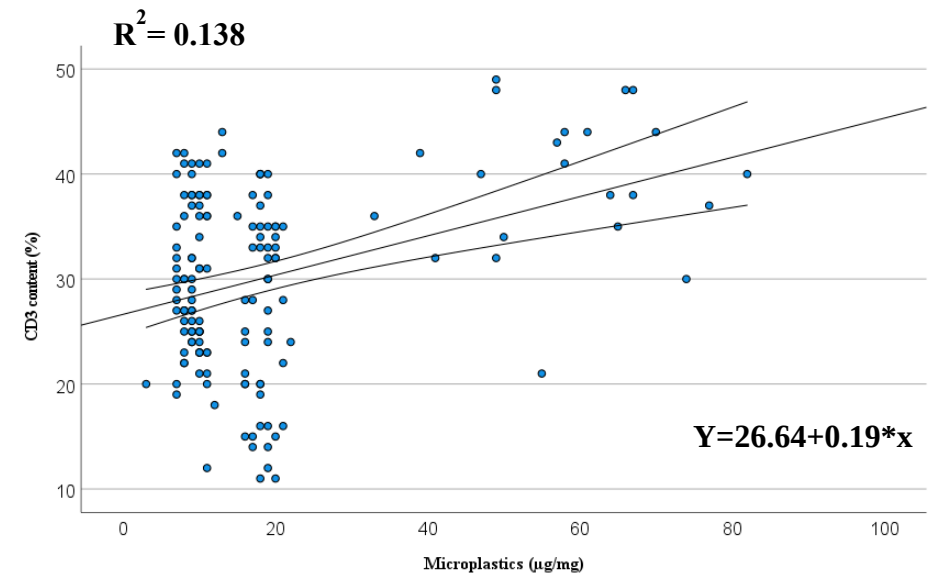

Linear regression analyses of the relationship between levels of micronanoplastics levels (μg/mg of plaque) and the expression of Interleukin (IL)-18, IL-1β, IL-6, and tumor necrosis factor (TNF)-α (pg/mg) measured by ELISA, or the expression of collagen, cluster of differentiation (CD)68, and CD3 contents (% of signal), measured by immunohistochemistry. Regression lines and the relative 95% confidence intervals lines are shown.

Figure S6. Expression of plaque markers in the three groups of patients without evidence of micronanoplastics in the plaque, with evidence of polytheylene only, or with evidence of both polyethylene and polyvinylchloride.

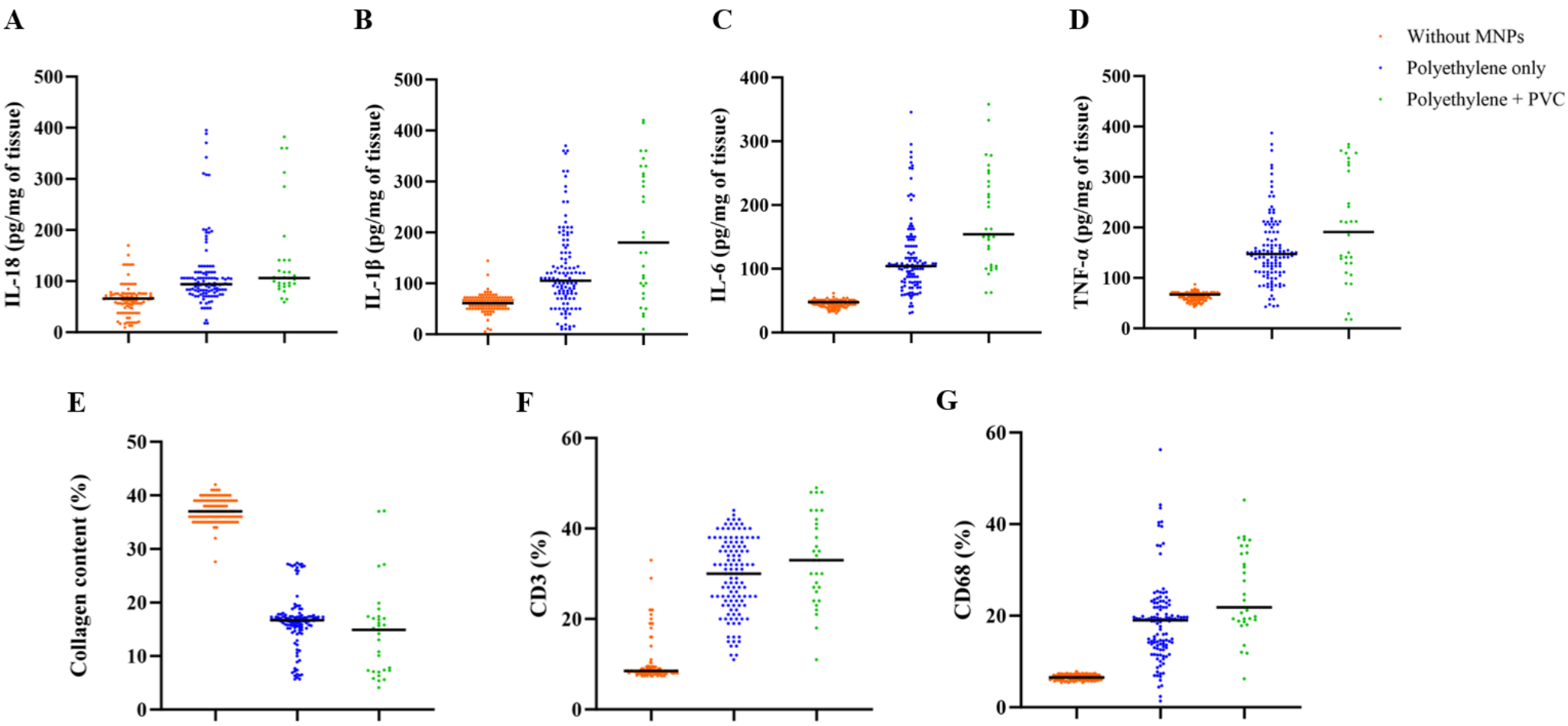

The abundance of Interleukin (IL)-18 (A), IL-1β (B), IL-6 (C), and tumor necrosis factor (TNF)-α (D) assessed by ELISA, and of collagen content (E), cluster of differentiation (CD)3 positivity (F), and CD68 positivity (G), measured by immunohistochemistry, in the three groups of patients without evidence of micronanoplastics within the plaque (n= 107), polytheylene only (n= 119), or with evidence of both polyethylene and polyvinylchloride (PVC) (n= 31). Mean and individual points are shown. MNPs denotes micro-nanoplastics.

Table S1. Baseline characteristics, prevalence of micronanoplastics positivity, and mean levels of micronanoplastics in excluded and included patients.

Variable	Included (n=257)	Excluded (n = 47)
Age (IQR) — yr	72 (66-77)	72 (68-75)
Male — no. (%)	194 (75.5)	35 (74.5)
Body-mass index*	28 (27-29)	28 (27-29.2)
Hypertension — no. (%)	147 (57.2)	24 (51.1)
Systolic blood pressure (IQR) — mmHg	125 (118-129)	125 (120-130)
Diastolic blood pressure (IQR) — mmHg	77 (75-85)	75 (70-85)
Heart rate (IQR) — bpm	81 (76-86)	85 (80-90)
Stenosis severity (IQR) — %	78 (73-83)	77 (75-80)
Diabetes — no. (%)	68 (26.5)	11 (23.4)
Cardiovascular diseases^{+} — no. (%)	86 (33.5)	16 (34)
Dyslipidemia — no. (%)	94 (36.6)	18 (38.3)
Total cholesterol (IQR) — mg/dl	150 (142-158)	149 (144-160)
LDL cholesterol (IQR) — mg/dl	75 (68.8-83.4)	70.2 (64.5-86.2)
HDL cholesterol (IQR) — mg/dl	42 (40-44)	42 (40-43)
Triglycerides (IQR) — mg/dl	179 (163-193)	184 (162-189.5)
Creatinine (IQR) — mg/dl	1 (1-1.1)	1 (0.9-1.1)
Smokers — no. (%)	40 (15.6)	8 (17)
Beta-blockers — no. (%)	82 (31.9)	15 (31.9)
ACE inhibitors — no. (%)	128 (49.8)	25 (53.2)
ARBs — no. (%)	66 (25.7)	12 (25.5)
Calcium channel blockers — no. (%)	21 (8.2)	4 (8.5)
Diuretics — no. (%)	33 (12.8)	7 (14.9)
Heparin — no. (%)	22 (8.6)	5 (10.6)
Antiplatelet drugs — no. (%)	251 (97.7)	45 (95.7)
Statin — no. (%)	244 (94.9)	44 (93.6)
Ezetimibe — no. (%)	46 (17.9)	7 (14.9)
Prevalence micronanoplastics (%)	150 (58.4)	27 (57.4)
MNPs level — µg/mg plaque	21.7±24.5	15.3±25.1

MNPs denotes micronanoplastics, mmHg millimeters of mercury, bpm beats per minute, LDL low-density lipoprotein, HDL high-density lipoprotein, ACE angiotensin converting enzyme, ARBs angiotensin II receptor blockers.

*Body-mass index is measured as kilograms per square meter. + Cardiovascular diseases are defined as a previous event of acute coronary syndrome.

Table S2. Incidence of individual components of the composite outcome in patients with and without micro-nanoplastics.

	Patients without micronanoplastics (n= 107)	**Patients with micronanoplastics (n= 150)**
Stroke — no.	5	14
Myocardial infarction — no.	2	10
All cause death — no.	1	6

Table S3. Cox regression analysis for the primary outcome.

Variables	Hazard Ratio (95% Confidence Interval)
Presence of MNPs	4.53 (2.00 – 10.27)
Age	1.04 (0.98 – 1.09)
Sex	0.55 (0.26 – 2.00)
Body-mass index*	0.82 (0.68 – 0.97)
Diabetes	4.76 (2.35 – 9.60)
Hypertension	1.37 (0.69 – 2.72)
Cardiovascular diseases^{+}	1.65 (0.80 – 3.41)
Total cholesterol	1.01 (0.97 – 1.04)
LDL cholesterol	0.96 (0.93 – 1.00)
HDL cholesterol	0.97 (0.86 – 1.09)
Triglycerides	1.01 (1.00 – 1.03)
Creatinine	0.30 (0.04 – 2.46)

Adjusted hazard ratios (HR) with the relative 95% confidence interval (CI) derived from the Cox regression analysis testing the association between the presence of MNPs and the primary outcome. Results for all the covariates added are shown. The relative cumulative incidence is shown in Figure 4.

*Body-mass index is measured as kilograms per square meter. + Cardiovascular diseases are defined as a previous event of acute coronary syndrome.

MNPs denotes micronanoplastics, LDL low-density lipoprotein, and HDL high-density lipoprotein.

Table S4. Cox regression analysis of the association of micro-nanoplastics levels as a continuous variable and the primary outcome.

Variables	Hazard Ratio (95% Confidence Interval)
Micronanoplastics (for 1 unit)	1.04 (1.03 – 1.04)
Age	1.02 (0.96 – 1.04)
Sex	0.58 (0.27 – 1.24)
Body-mass index*	0.80 (0.68 – 0.95)
Diabetes	3.08 (1.46 – 6.48)
Hypertension	0.70 (0.34 – 1.42)
Cardiovascular diseases^{+}	1.27 (0.59 – 2.76)
Total cholesterol	1.01 (0.98 – 1.03)
LDL cholesterol	0.99 (0.95 – 1.03)
HDL cholesterol	0.96 (0.84 – 1.09)
Triglycerides	1.01 (1.00 – 1.03)

Adjusted hazard ratios (HR) with the relative 95% confidence interval (CI) derived from the Cox regression analysis testing the association between MNPs levels as a continuous variable and the primary outcome. Results for all the covariates added are shown. *Body-mass index is measured as kilograms per square meter. + Cardiovascular diseases are defined as a previous event of acute coronary syndrome.

LDL denotes low-density lipoprotein and HDL high-density lipoprotein.

Table S5. Representativeness of Study Participants.

Category	Comment
Disease, problem, or condition under investigation	Association between the presence of micronanoplastics in the carotid plaque and the incidence of major adverse cardiovascular events
Special considerations related to	
Sex and gender	The general incidence of cardiovascular diseases is higher in men than in women, a notion that applies also to patients with carotid stenosis. Preliminary data suggest that women might suffer more the cardiovascular consequences of exposure to selected pollutants, *e.g*. PM 2.5, but such information is not available for micronanoplastics.
Age	The incidence of cardiovascular diseases increases with age, both in the general population and in patients with carotid stenosis. Old age, *i.e.* > 80 years, reverses the pattern of increased risk seen in men vs women. Age might interact with specific pollutants, *e.g*. PM 2.5, when assessing cardiovascular outcomes, but these data are not available for micronanoplastics.
Race or ethnic group	Black people have a higher burden of cardiovascular diseases. Blacks, Asians, Hispanics, Latinos, and low-income populations are exposed to higher levels of fine particulate air pollution and could suffer more the noxious effects of pollution, but data of exposure to micronanoplastics are missing.
Geography	There is a consistent heterogeneity across the globe in terms of incidence of cardiovascular diseases and exposure to pollutants. Specific information relative to micronanoplastics is lacking.
Other considerations	Albeit data for microplastics are scarce, the association between pollution and poor health outcomes is suggested to be influenced by income level. A disadvantaged social status increases the chances of suffering the consequences of air pollution.
Overall representativeness of this study	In the present study, men were more represented than women in both groups with and without evidence of nanomicroplastics, in line with the general population. Sex was established according to what was reported in the identity card. Gender was not investigated. The age range was relatively restricted with 75% patients having from 65 to 77 years, consistent with the population usually approaching the clinic for carotid stenosis. All patients were of Caucasian origin and lived in the south of Italy. Thus, findings may not apply to other geographical areas or ethnicities. Information relative to social status was not collected.